TÜBİTAK

Turk J Phys
34 (2010) , 33 – 42.

doi:10.3906/fiz-0903-10

Sublimation of graphite in continuous and pulsed arc discharges

Afshan ASHRAF[1,2], Kashif YAQUB[1,2], Sumera JAVEED[1,2], Sumaira ZEESHAN[1,2]
Rahila KHALID[1], Sohail Ahmad JANJUA[1] and Shoaib AHMAD[1]
[1] *Accelerator and Carbon Based Nanotechnology Laboratory-PINSTECH*
e-mail: subahyaqeen@gmail.com
[2] *Pakistan Institute of Engineering and Applied Sciences (PIEAS)*
P. O. Box Nilore, Islamabad-PAKISTAN

Received 23.03.2009

Abstract

Sublimation of graphite has been investigated in continuous and pulsed arc discharges. The results of continuous arc discharge between graphite electrodes are compared with pulsed arc discharge between cylindrical Aluminum cathode and annular graphite anode. The sublimed species include monoatomic and diatomic carbon clusters with their relative composition depending upon the mechanism of energy dissipation in graphite electrodes. Diatomic carbon (C_2) is the dominant subliming cluster. Emission spectroscopy of the Swan band system $[d^3\prod_g - a^3\prod_u]$ of C_2 has been used to investigate the thermodynamic state and to deduce the vibrational temperature (T_{vib}). The vibrational level densities indicate that local thermodynamic equilibrium exists in both types of discharges and $T_{vib} \approx$ 7000–9000 K.

Key Words: Graphite sublimation, continuous arc discharge, pulsed arc discharge, electron collision.

PACS: 81.05Uw; 64.70.Hz; 52.80.Mg; 52.20Fs.

1. Introduction

In the present investigation, phenomenon of sublimation of graphite anode has been studied in two discharge geometries. One is conventional continuous arc discharge and the other is pulsed arc discharge in cylindrical geometry. These sources have been operated in non-regenerative sooting discharge mode, in which soot is produced and either removed from the location of its production or deposited on a cool substrate. On the other hand, in regenerative sooting discharges, soot re-establishes itself on the cathode surface. The kinetic and potential sputtering, collisions with energetic electrons and with other constituents of discharge, causes this soot to regenerate. [1]. Therefore, there is a subtle difference in the production of carbon clusters in such

a regenerative environment, one in which sublimation dominates (in non-regenerative mode). In continuous arc discharge removal of surface constituents of graphite anode is characterized by sp^2 bond breaking due to thermal energy provided by electrons. Emission of monatomic, diatomic and larger carbon clusters C_x ($x \geq 3$) occurs due to the sublimation of graphite anode.

C_2 has unique properties and plays an important role in the formation and fragmentation processes leading to closed cage carbon clusters. Our theoretical studies have highlighted the role of C_2 in self-assembly of fullerenes and single walled nanotubes [2, 3].

The continuous arc discharge method reported here is similar to that used by Krätschmer et al. [4]. In this technique, cathodic thermal emission of electrons provides the high current density necessary to heat and sublime the anode. The subliming electrode material is excited and ionized by electrons and emits characteristic spectral radiation. Arc discharges are operated from atmospheric pressures down to about 10 Torr with voltage $\sim$20 V and current up to 100 A [5]. Helium is used in the chamber because it has better thermal conductivity, which is an essential requirement in the present case to remove excess heat, and to operate the source for longer periods of time. The first excited level for helium is above the operating voltage in the present work, which ensures that no emission line from helium arises, hence simplifying the spectrum under observation.

A new pulsed arc discharge technique that uses electron pulse for sublimation of graphite is presented, which is characteristically different from the carbon plasma produced by laser ablation. Differences in the two types of sooted vapors are in varying relative densities of C_1, C_2, C_3 and larger radicals depending on experimental parameters. In laser ablation, large amount of electromagnetic power is delivered to spots of millimeter dimensions. [6]. Bonds are broken only in the target area and localized surface erosion occurs in ablated targets. The pulsed sublimation mechanism utilizes the geometry of Z-pinch plasma ion source such as that developed by the ZaP experimental group. The ZaP team developed the technique to achieve high temperature densities for fusion reactions [7, 8]. We use the ZaP geometry only and are not, however, aiming at high temperature and electron density conditions as in the conventional Z-pinch experiments. Sugai et al. [9] also used pulsed arc discharge to synthesize double walled carbon nanotubes inside a high temperature furnace at 1000–1400 °C. But we produced pulsed arc discharge at room temperature. Pulsed arc discharge operation has certain similarities with that of laser ablation by Kroto et al. [10], in which laser pulse width of the order of nanosecond was used to ablate rotating discs of graphite. In case of laser ablation, photons deliver energy in electromagnetic-charged particle interaction, while in electron pulsed mode energy is transferred by electron-electron collisions occurring over pulse width $\sim$200 μs. The electron pulses can also deliver hundreds of kilowatt which may be comparable with megawatt energy levels delivered in laser pulses. Electron pulses, however, are distributed over the entire target surface, while the laser pulse is focused to a fraction of the surface area. In each of the two interactions, bond breaking of the target atoms takes place and sublimation of solids proceeds. Ne is selected because it has lower ionization potential than He and we need to ionize the gas in pulsed arc to get sufficient number of electrons available to produce electron pulse hitting the graphite cathode, which ultimately sublime the material.

2. Experimental

The experimental setups are shown in Figure 1. These setups were used to study the sublimation process in continuous and pulsed arc discharges, using gasses He and Ne as support gases, respectively. Emission

spectroscopy is applied to study the state of excitation of sublimed atoms and clusters in both cases and to evaluate whether the ensuing plasmas are in local thermodynamic equilibrium (LTE) or not.

2.1. Continuous arc discharge

Continuous arc discharge was produced at 20 V and 50 A between graphite electrodes in the presence of He at 50 mbar. The arc discharge is initiated by touching the electrodes. Once discharge stabilizes, the electrodes are withdrawn to a distance of nearly 2 to 3 mm. The setup is shown in Figure 1(a).

The diameter of graphite electrodes is 10 mm and length 70 mm. High current flows through the electrodes and temperature of electrode $\gtrsim$ 3000 K.

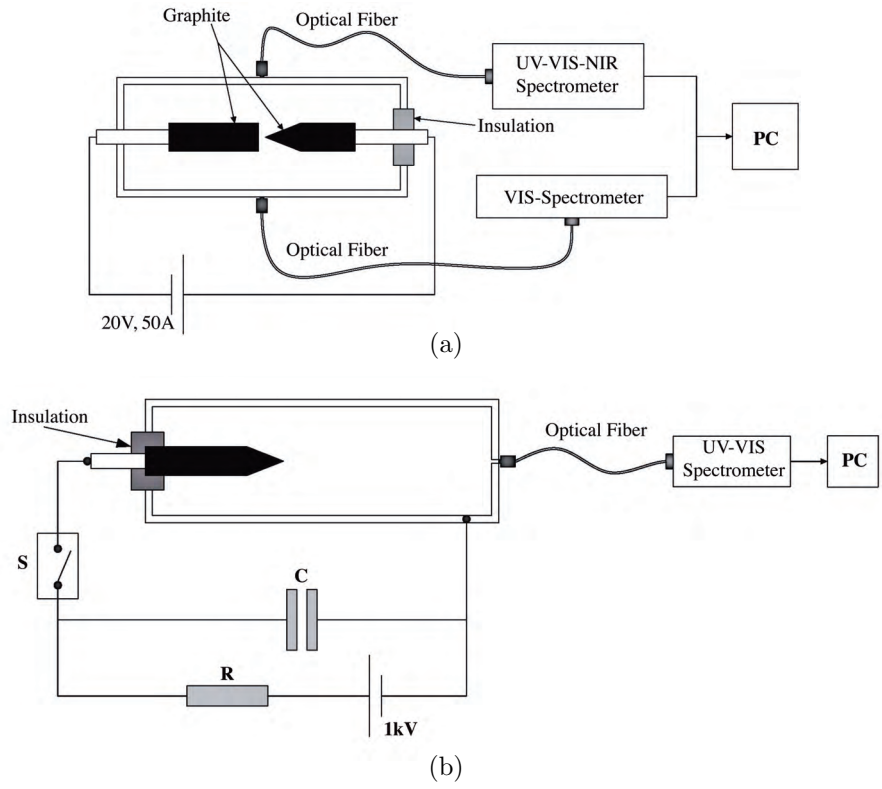

Figure 1. Schematic of the experimental setup used for study of sublimation in (a) continuous arc discharge, (b) pulsed arc discharge.

2.2. Pulsed arc discharge

The experimental setup is shown in Figure 1(b). A voltage pulse of nearly 1 kV applied through a capacitor generates a pulsed arc discharge between electrodes in the presence of Ne at 0.2 mbar. The anode was composed of graphite, of 15 mm diameter, 70 mm length, surrounded by cylindrical aluminum cathode of 30 mm diameter and 300 mm length. Radial separation between electrodes is 17 mm. Charged particles produced in the discharge and those provided by cathode are forced to assemble in a cylindrical geometry by $E \times B$ force. Energized electrons hitting the anode tip caused it to sublime.

Time constant of the capacitor charging circuit is 25 s. The source is operated in pulsed mode with pulse width $\sim$200 μs and the discharge occurs at every 30^{th} second. Energy transferred per pulse is $\sim$5 J. Emission spectrum is taken through the front aperture.

2.3. Emission spectroscopy

Emission spectroscopy of the two types of discharges is performed by CCD based visible (Vis) (400-600 nm) and ultraviolet-visible-near infrared (UV-Vis-NIR) (200–1100 nm), using Ocean optics spectrophotometers. The UV-Vis-NIR spectrophotometer has resolution $\sim$1 nm with broad wavelength range in which one can get a good picture of overall discharge while Vis spectrophotometer has higher resolution $\sim$0.16 nm with shorter range to especially identify and analyze C_2 Swan band $[d^3\prod_g - a^3\prod_u]$ [11]. Photon intensities I are calibrated using differential curves $\mathrm{d}I/\mathrm{d}\lambda$ in units of μW/cm^2 -nm. The calibration was done using an Ocean Optics DH-2000 Halogen light source and irradiance software. The calibrated intensity I can be used to obtain the upper level population densities in units of cm^{-3}.

3. Results and discussion

The emission spectrum obtained from continuous arc discharge is shown in Figure 2(a). The most prominent feature of this spectrum is the C_2 Swan band system $[d^3\prod_g - a^3\prod_u]$, $\Delta\nu$ = 0, +1, -1. Absence of He lines is another feature of this spectrum. The role of Helium as a gaseous coolant in graphite arc discharges has been discussed by Gamely and Ebbesen [12]. Therefore, He is utilized efficiently for thermal cooling of carbon vapour prior to condensation.

A similar emission spectrum, obtained from the pulsed arc discharge, is shown in Figure 2(b). In addition to the C_2 Swan band, there are some Ne lines (NeI 585, 588 nm) as well. A very strong H I peak is seen at 486 nm. Plasma established between anode tip and cathode is found to be rich in sublimed C_2. A smaller fraction of C I, C II and C III is also detected but only in the pulsed mode.

Level density N_u of the upper excited levels (electronic or vibrational) can be obtained from emission spectrum by using the following equation:

$$I_{ul} = N_u A_{ul} h\upsilon_{ul}, \tag{1}$$

where I_{ul} is the calibrated intensity obtained from spectrum for relevant transition, $h\nu_{ul}$ is energy difference between upper (u) and lower (l) levels and A_{ul} is the Einstein transition probability of spontaneous emission for selected transition [13]. The spectrum is background subtracted and calibrated against the experimental setup. Linear baseline correction is also applied to resolve the relevant peaks. The T_{vib} is calculated using the Boltzman relation

$$N_u = \frac{g_u N}{U(T)} \exp\left(-\frac{E_u}{k_B T_{vib}}\right), \tag{2}$$

where N is the total density of particles, g_u is the statistical weight of the upper state, $U(T)$ is the atomic or molecular internal partition function, and E_u is the energy of the upper level relative to the ground state. A range of upper level densities for $\Delta\nu$ = 0, +1, -1; is calculated from the emission spectrum. By plotting $\ln\left(\frac{N_u}{g_u}\right)$ as a function of E_u, one can determine T_{vib} from slope of the graph (-1/$k_B T_{vib}$) [14]. The population

inversion parameter (PIP) is defined by $PIP = \left[\frac{N_u g_l}{N_l g_u}\right]$. If $PIP < 1$, for all the levels involved in the transition, the plasma is in LTE and Boltzmann relation is valid [15].

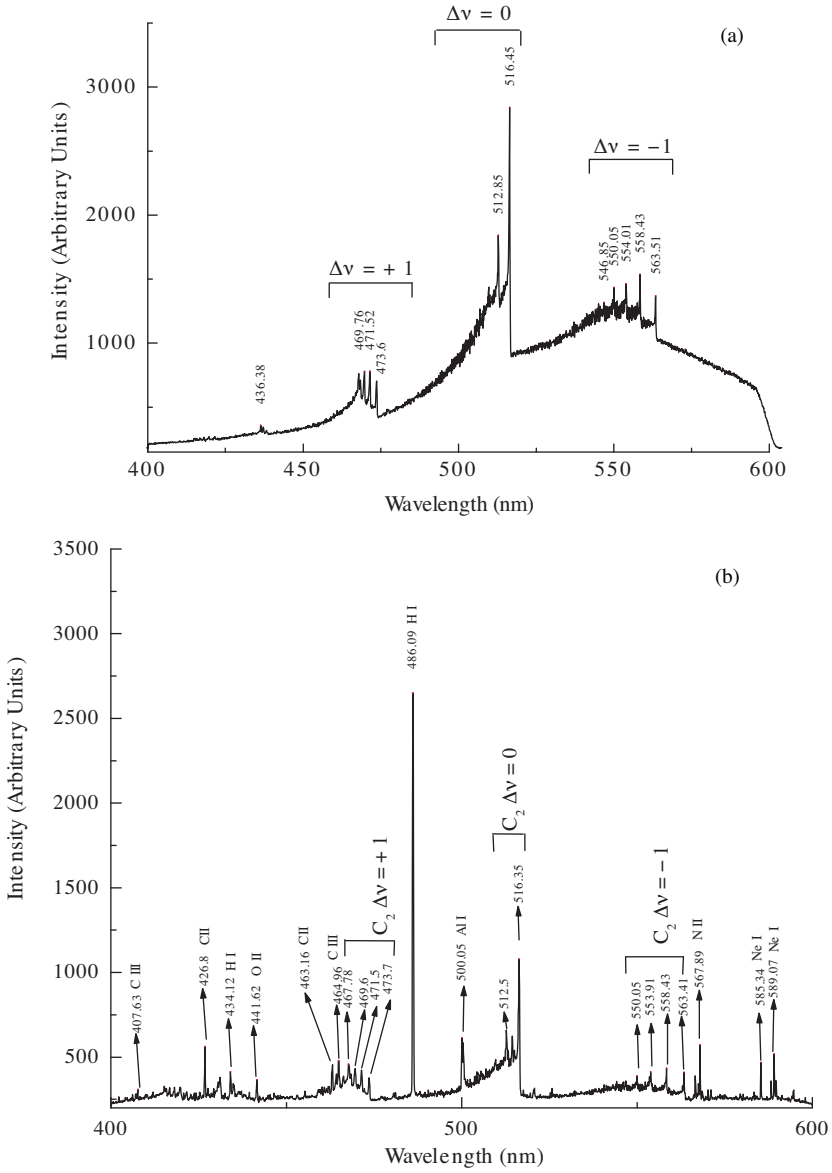

Figure 2. C_2 Swan band in (a) emission spectrum obtained from continuous arc discharge, (b) emission spectrum obtained from pulsed arc discharge.

3.1. Continuous arc discharge

The plot of average level densities of four vibrational levels of excited $C_2(\nu\prime = 0, 1, 2, 3)$, obtained from a set of experiments, is shown in Figure 3(a). The number density N_u of $\nu\prime = 0$ is an average of two transitions, i.e. ($0 \rightarrow 1$; at 563 nm) and ($0 \rightarrow 0$; at 516 nm). The number density N_u of $\nu\prime = 1$ is an average of transition

(1→0; at 473 nm) and transition (1→2; at 558 nm). The number density N_u of $\nu\prime = 2$ is an average of transitions (2→1; at 471 nm) and (2→3; at 554 nm). Similarly, the N_u of $\nu\prime = 3$ is an average of transitions (3→2; at 469 nm) and (3→4; at 550 nm). It is evident from Figure 3(a) that level densities follow Boltzmann distribution, as the higher vibrational levels are less populated than lower ones. The small variation in the last two points is due to low number densities, which could not be treated as population inversion, as the variations are within error limits.

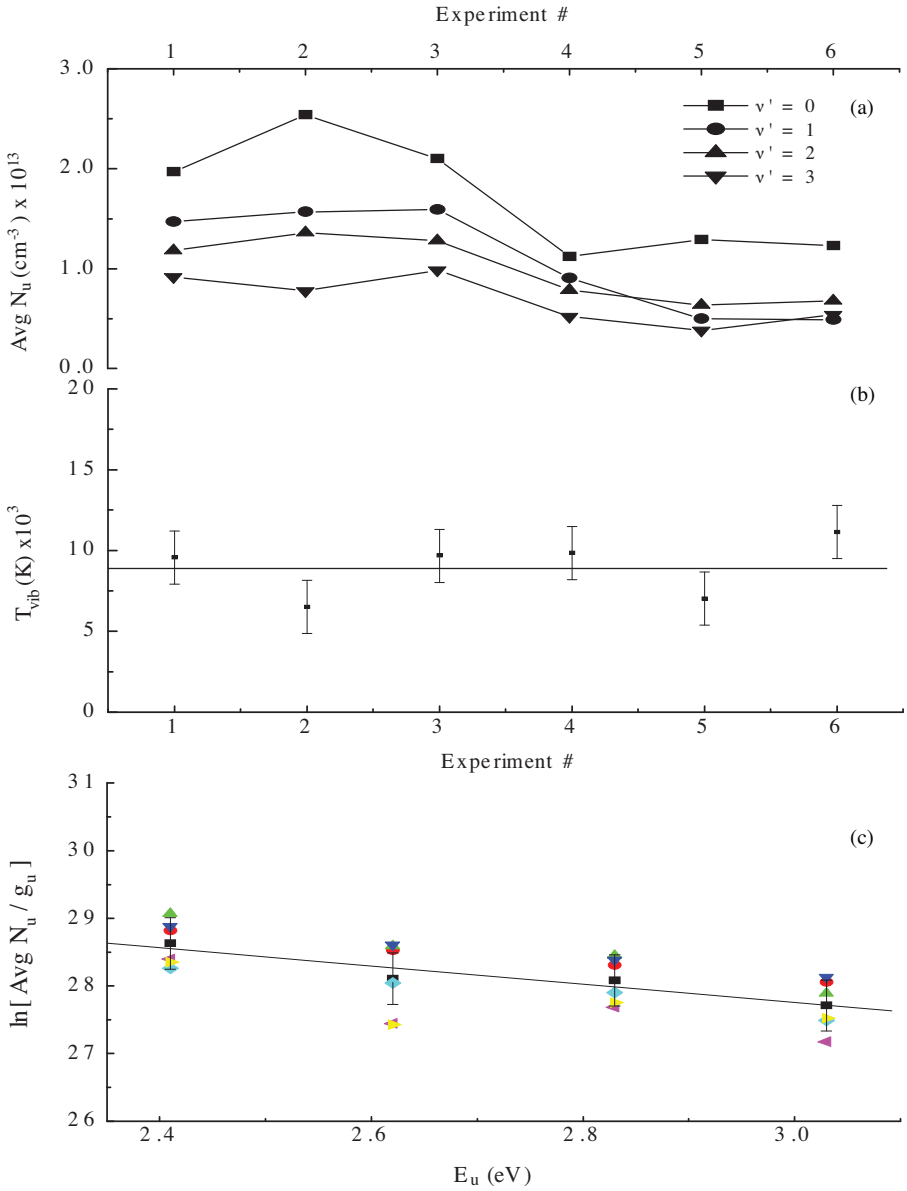

Figure 3. (a) Plot of average level densities of four vibrational levels of excited C_2 ($\nu\prime = 0$, 1, 2, 3) obtained from continuous arc discharge. (b) Plot of T_{vib} obtained from set of experiments using average number densities (N_u) of excited C_2. (c) Graph of $\ln(\mathrm{Avg}\, N_u / g_u)$ for C_2 from set of experiments as a function of E_u (related to $\nu\prime = 0$, 1, 2, 3).

The T_{vib} = 8960 K ± 1600 K obtained from the set of experiments is shown in Figure 3(b). The plot of $\ln\left(\frac{N_u}{g_u}\right)$ from the set of experiments versus E_u (related to $\nu\prime$ = 0, 1, 2, 3) is shown in Figure 3(c). Taking the average of $\ln\left(\frac{N_u}{g_u}\right)$ corresponding to $\nu\prime$ = 0, 1, 2, 3, and applying Boltzmann slope method, gives T_{vib} = 8630 K ± 2000.

3.2. Pulsed arc discharge

The behavior of averaged number densities of C_2 for the set of experiments is shown in Figure 4(a). Pulsed discharge has a distinct feature that it includes atomic and ionized carbon (C I, C II, C III). The excited states of Ne I (585, 588 nm), H I (434, 486 nm), Al I (500 nm) are also seen. Following the same procedure as for Figure 3(b), the averaged value of T_{vib} = 8037 K ± 1320 and is shown in Figure 4(b).

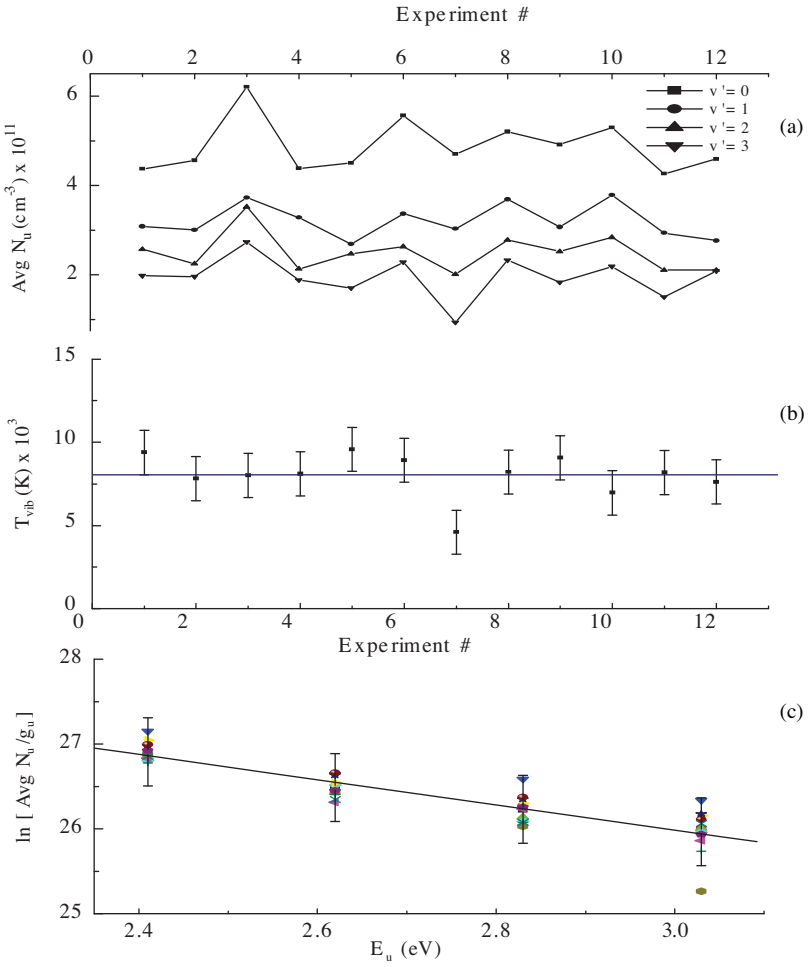

Figure 4. (a) Plot of average level densities of four vibrational levels of excited C_2 ($\nu\prime$ = 0, 1, 2, 3) obtained from set of experiments performed using pulsed arc discharge. (b) Plot of T_{vib} obtained from set of experiments using average number densities (N_u) of excited C_2. (c) Graph of $\ln[\mathrm{Avg}N_u/g_u]$ for C_2 from set of experiments as a function of E_u (related to $\nu\prime$ = 0, 1, 2, 3).

The averaged number densities of $\nu\prime = 0,1,2,3$ were deduced by following the same procedure as described in section 3.1. The T_{vib}= 7814 K $\pm$ 670 thus calculated is shown in Figure 4(c).

Characteristic emission from triplet-excited states of the Swan band has provided important and essential clues about the state of excitation and relative population densities of C_2 in the above-mentioned experiments.

Figure 5 shows the total number densities of C_2, CII and CIII, which have been calculated by adding number densities corresponding to all transitions in each experiment. For C_2, we have calculated number density by taking 467.78, 469.6, 471.5, 473.7, 512.5, 516.35, 550.05, 553.91, 558.43 and 563.41 nm transitions. For CII, we have calculated total number density by taking 426.8, 463.16; and for CIII, 407.63 and 464.96 nm transitions. In addition to direct sublimation, CII and CIII may also be produced by disintegration of C_2 and due to fragmentation of higher clusters. However, the amount of CII is higher than CIII, due to difference in the ionization potentials. The average number densities obtained for C_2, CII and CIII are 4.66×10^{12}, 6.96×10^{11}, and 1.84×10^{11} cm^{-3}, respectively. The order of magnitude higher number density of C_2 indicates that it plays the role of sublimation process precursor.

From Figures 3 and 5, the C_2 yield for continuous arc discharge is $\sim5\times10^{13}$ cm^{-3}, and $\sim5\times10^{12}$ cm^{-3} for pulsed arc discharge. Thus, for fullerene synthesis, continuous arc is likely to give 10 times better yield than for pulsed arc.

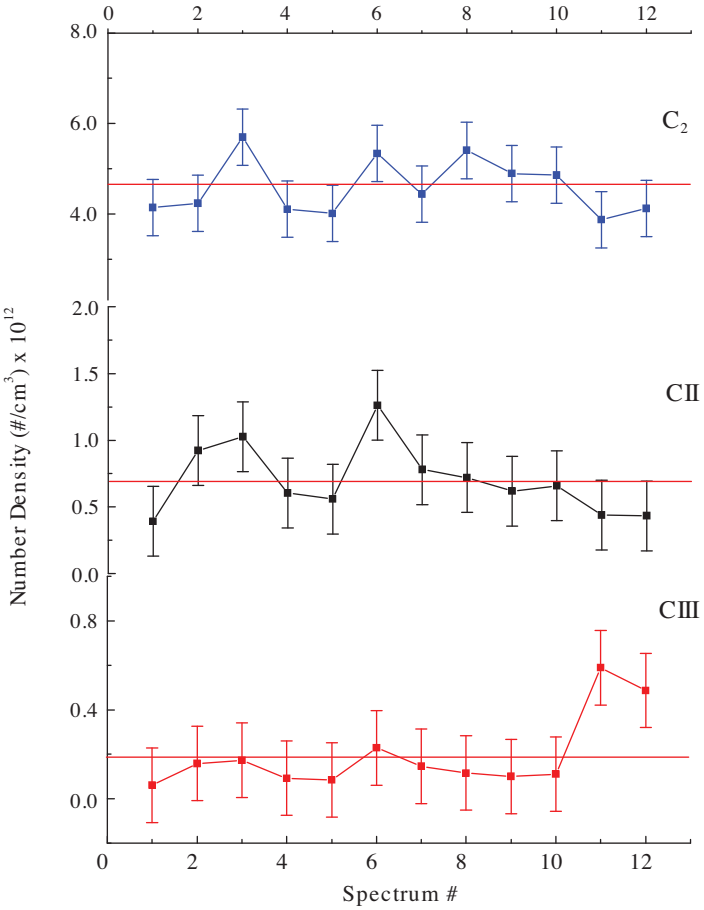

Figure 5. Intensities of C_2, CII and CIII plotted for set of pulsed arc discharge experiments.

4. Conclusions

Two experimental configurations for continuous and pulsed arc discharges have been used to study the mechanisms of sublimation. In both cases predominant emission of C_2 from graphite anode has been observed. In pulsed mode a smaller fraction of C_1 in atomic and ionized state is detected additionally, but it is absent in the emission spectra from continuous arc discharge. So it can be said that C_2 disintegration is prominently observed in pulsed arc, but not in continuous arc discharge. Resistive heating of electrodes may be responsible for the appearance of blackbody continuum in spectra of continuous arc. Blackbody continuum is not observed in pulsed arc. Continuous and pulsed arc discharges have similar range of vibrational temperatures (7000–9000 K). In both cases, C_2 is prominent sublimed species and carry most of the energy transferred to the graphite electrode. Hence the presence of C_2 acts as precursor for sublimation process. Also, continuous arc is better than pulsed arc as far as fullerene synthesis is concerned. Therefore, we conclude that the two techniques can alternatively be utilized for sublimation. There is an advantage in pulsed sublimation, as one can control the rate of sublimation by appropriate choice of pulsing parameters. This technique may be useful for controlled growth of carbon thin films.

Acknowledgements

The authors gratefully acknowledge technical support provided by Mr. Rizwan, Mr. Faisal and GSD workshops for fabrication of different components. We also acknowledge Mr. Abdul Hamid for providing us high voltage and high capacity capacitors.

References

[1] S. Ahmad, *Eur. Phys. J. D*, **18**, (2002), 309.

[2] S. Ahmad, *Nanotechnology*, **16**, (2005), 1739.

[3] S. Ahmad, S. D. Khan, S. Manzoor, *Nanotechnology*, **17,** (2006), 1686.

[4] W. Kratschmer, L. D. Lamb, Fostiropoulous, D. R. Huffman, *Nature*, **347**, (1990), 354.

[5] D. Williams, *Methods of Experimental Physics*. vol. 13, Part A, (Academic Press, New York. 1976).

[6] E. A. Rohlfing, D. M. Cox, A. Kaldor, *J. Chem. Phys*, **81,** (1984), 3322.

[7] K. A. Munson, U. Shumlak, B. A. Nelson, *American Physical Society* 48th annual DPP meeting, (University of Washington. 2006).

[8] U. Shumlak, R.C. Lilly, C. S. Adams, R. P. Golingo, S. L. Jackson, S. D. Knecht et al, 42^{nd} *AIAAA/ASME/ SAE/ ASEE Joint Propulsion Conference, Sacramento,* (California. 2006).

[9] T. Sugai, H. Yoshida, T. Shimada, T. Okazaki, and H. Shinohara, *Nano lett.*, **3**, (2003), 769.

[10] H. W. Kroto, J. R. Heath, S. C. O'Brien, R. F. Curl, R. E. Smalley, *Nature*, **318**, (1985), 162.

[11] R. W. B. Pearse, A. G. Gaydon. *The Identification of Molecular Spectra*, 4^{th} edition, (John Wiley & Sons, Inc., New York.1976).

[12] E. G. Gamaly, T. W. Ebbesen, *Phys. Rev. B*, **52,** (1995), 2083.

[13] I. I. Sobelman, *Introduction to the Theory of Atomic Spectra*, D. ed. T. Har, *International series of monographs in natural philosophy,* vol. 40, (Pergamon Press. Oxford. 1972).

[14] M. Venugopalan, *Reactions under Plasma Conditions*, vol. 1, (John Wiley, New York. 1971).

[15] E. B. Vitense, *Introduction to Stellar Astrophysics*, vol. 2, (Cambridge university Press, New York. 1993).